PREVENTION OF THE 2/1 NEOCLASSICAL TEARING MODE IN DIII-D

by
R. PRATER, R.J. LA HAYE, T.C. LUCE, C.C. PETTY, E.J. STRAIT, J.R. FERRON,
D.A. HUMPHREYS, A. ISAYAMA, J. LOHR, K. NAGASAKI, P.A. POLITZER, M.R. WADE,
and A.S. WELANDER

OCTOBER 2006

GENERAL ATOMICS

DISCLAIMER

GA–A25575

PREVENTION OF THE 2/1 NEOCLASSICAL TEARING MODE IN DIII-D

by
R. PRATER, R.J. LA HAYE, T.C. LUCE, C.C. PETTY, E.J. STRAIT, J.R. FERRON,
D.A. HUMPHREYS, A. ISAYAMA,[*] J. LOHR, K. NAGASAKI,[†] P.A. POLITZER, M.R. WADE,
and A.S. WELANDER

*Japan Atomic Energy Agency, Naka, Japan.
†Institute of Advanced Energy, Kyoto University, Kyoto, Japan.

GENERAL ATOMICS PROJECT 30200
OCTOBER 2006

GENERAL ATOMICS

Prevention of the 2/1 Neoclassical Tearing Mode in DIII-D

R. Prater 1), R.J. La Haye 1), T.C. Luce 1), C.C. Petty 1), E.J. Strait 1), J.R. Ferron 1),
D.A. Humphreys 1), A. Isayama 2), J. Lohr 1), K. Nagasaki 3), P.A. Politzer 1),
M.R. Wade 1), and A.S. Welander 1)

1) General Atomics, San Diego, California, USA
2) Japan Atomic Energy Agency, Naka, Japan
3) Institute of Advanced Energy, Kyoto University, Kyoto, Japan

e-mail contact of main author: prater@fusion.gat.com

Abstract. Onset of the m/n = 2/1 neoclassical tearing mode (NTM) has been prevented in high-performance DIII-D discharges using localized electron cyclotron current drive (ECCD). Active tracking of the $q = 2$ surface location, using real-time equilibrium reconstructions with motional Stark effect data, allows the current drive to be maintained at the rational surface even in the absence of a detectable mode. With the application of this technique in DIII-D hybrid discharges, the 2/1 mode is avoided and good energy confinement is maintained for more than 1 second with β at the estimated n = 1 no-wall stability limit for ideal kink modes (β_T approximately equals 3.9% and normalized beta β_N approximately equals 3.2). The results can be understood through modeling using the modified Rutherford equation.

1. Introduction

High fusion gain in a tokamak requires operation near the pressure limit for stability. An instability that places a limit on the pressure is the neoclassical tearing mode, which may arise when the normalized plasma pressure $[\beta_N \equiv \beta / (I_{MA}/a_m B_T)]$ exceeds a critical value. For ITER, β_N is 1.84, which is well below the no-wall β limit and well above the expected neoclassical tearing mode (NTM) β limit [1]. Relief from the lower β limit will permit higher performance operation in ITER. In this paper we show that the NTM may be avoided by application of electron cyclotron current drive (ECCD) and β_N subsequently raised to the estimated no wall stability limit ($\beta_N = 3.2$).

The NTM is a magnetic island that is caused by a perturbation to the plasma current of the same helicity as the field line on a rational flux surface. Perturbations with poloidal mode number m=3 and toroidal mode number n=2 degrade the energy confinement by typically 10% to 30%, while perturbations with m=2/n=1 can lead to severe energy loss and disruption. The 2/1 mode occurs at the minor radius where the safety factor $q = 2$, which is close to the plasma boundary, so the interaction of the magnetic perturbation of the mode with induced eddy currents in the vacuum vessel leads to reduction of the plasma rotation, which in turn leads to mode locking and likely to a disruption [2]. An estimate for ITER of the size of the 2/1 magnetic island that causes locking is 5 cm, only 2.5% of the minor radius [1].

Theoretical work showing that ECCD placed accurately on the resonant surface can suppress NTMs [3,4] has led to successful experimental validation of this process for the 3/2 [5-7] and 2/1 [8,9] modes. In those experiments an NTM of fully saturated island size was suppressed by the ECCD. In some cases it was shown that this leads to operation at increased β [10,11]. This work has generally shown good agreement with theory [2]. The very narrow current drive profiles characteristic of ECCD in DIII-D [typically 4 cm Full Width Half Maximum (FWHM)] are well suited for this purpose, and the spatial precision of the placement relative to the rational surface is required to be of order 1 cm. Correct placement of the ECCD in the

island is facilitated by a feedback-controlled search technique to find the current drive location that minimizes the mode amplitude [8].

The process of locking and disruption can take place rather rapidly and at rather small island size. In order to avoid the potential disruption, it is preferable to avoid the 2/1 NTM entirely rather than to suppress the mode after it has grown to observable size. Theory suggests that this may be done in the absence of the island by applying current drive on the rational surface [12] in order to modify the classical stability parameter Δ' [13]. Experiments applying ECCD with this approach on JT-60U showed that the 3/2 mode could be avoided using less EC power than that which was required to stabilize the mode from its fully saturated state [14], but increased plasma pressure was not demonstrated in those experiments. Experiments on the preemptive stabilization of the 3/2 mode in DIII-D showed that higher stable β could be achieved [11].

In this paper, we present experiments on DIII-D in which the 2/1 NTM was completely avoided by application of ECCD at the $q = 2$ surface, which is more difficult than the 3/2 mode due to less effective current drive at the larger minor radius and to larger growth rate. These experiments show that the plasma β can be raised to at least the no-wall $n = 1$ kink mode beta limit, $\beta_N = 3.2$, for many confinement times without the mode occurring. One practical aspect of this approach is that in the absence of the NTM island there is no clear identifier of the location of the rational surface, and in practice the location of the rational surface changes as the plasma pressure is increased. To address this, reconstructions of the plasma equilibrium in real time are performed on DIII-D to identify the location of the rational surface as it moves. These reconstructions include measurements of magnetic field pitch angles from the motional Stark effect diagnostic. Real time control of the plasma position or of the toroidal field using the digital Plasma Control System (PCS) has been successful in keeping the ECCD sufficiently close to the rational surface that the mode is avoided.

2. Experiment

The experiments on DIII-D on avoiding the 2/1 NTM by means of ECCD at the $q = 2$ surface were performed in "hybrid mode" discharges. The hybrid mode is characterized by the presence of a small 3/2 NTM which acts to limit the central peaking of the current density profile but which is of sufficiently small size that the small confinement penalty is acceptable. By this means, the profile of current density is broadened, the sawtooth instability is avoided and improved performance is found.

In the present discharges, the 2/1 NTM is avoided altogether by application of ECCD at the rational surface. The H-mode discharge has a single-null divertor configuration with plasma current 1.2 MA, toroidal field 1.5 T, $q_{95} = 3.9$, and $\beta \approx 3.9\%$. The 110 GHz electron cyclotron heating (ECH) power is launched with x-mode polarization from a port above the midplane, and the second and third harmonics of the electron cyclotron resonance are shown. The total ECH power from four gyrotrons incident on the plasma is 2.4 MW. The EC power is launched with a toroidal angle of 14 deg from radial in a compromise between maximum ECCD (large toroidal angle) and minimum profile width (small toroidal angle). For these conditions, the full width at half maximum of the ECCD profile is about 5.6% in normalized minor radius, or 3 to 4 cm. The time-averaged neutral beam injection (NBI) power is under the real-time control of the PCS using a feedback system to keep the plasma β near a pre-programmed trajectory in time.

The geometry is shown in Fig. 1 and the radial profiles are shown in Fig. 2. The EC quantities are calculated by the TORAY-GA ray tracing code. Figure 1 shows that there is observable refraction of the EC waves away from the center of the plasma. Moderate refraction is expected since the electron density is $4 \times 10^{19}\,\mathrm{m}^{-3}$ at the minimum minor radius of the waves, about $\rho = 0.5$, is not small compared to the cutoff density of $6.4 \times 10^{19}\,\mathrm{m}^{-3}$ for 110 GHz and the value of the parallel index of refraction ($n_\parallel = 0.35$) there. The effects of wave refraction on the location of the current drive can be estimated by the PCS using a simple model based on real-time measurements of line-averaged density by two interferometers, one of which views the plasma radially near the midplane and one of which views the plasma vertically 27 cm inboard of the magnetic axis. For the geometry of Fig. 1 and the density in these experiments, the minor radius of the current drive is not very sensitive to refraction, and this system was not used in these experiments.
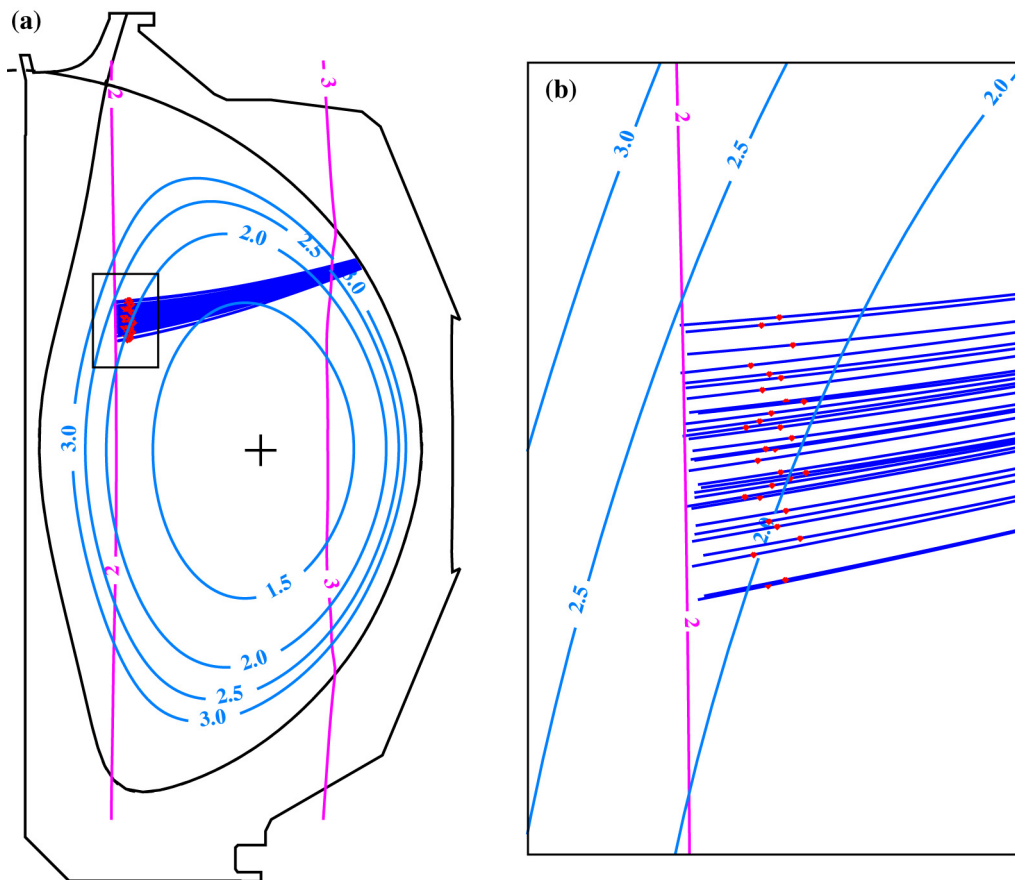

FIG. 1. Cross-section of the DIII-D discharge showing the rational q surfaces. The rays of the EC beam are shown as the blue lines, and the magenta lines marked 2 and 3 are the second and third harmonics of the electron cyclotron resonance. Rational q-surfaces are shown. (b) Expanded region of (a) showing relationship of the rays to the q surfaces. The red dots are at the location of maximum rate of attenuation, and the peak current drive is located along the ray a little closer to the antenna.

The geometry of Fig. 1 was chosen to facilitate movement of the location of the ECCD relative to the rational surface through small changes in the toroidal field under the control of the PCS. Increasing B_T increases the major radius of the second harmonic resonance, moving the ECCD to smaller minor radius. The third harmonic lies well inside the plasma, and approximately 60% the EC power is lost there parasitically. By coincidence the minor radius of the power lost at the third harmonic is near the minor radius of the second harmonic deposition, and this third harmonic power causes the broad wings on the profile of power

density in Fig. 2(d). Current drive by the third harmonic power is negligible because the resonant interaction is almost entirely with deeply trapped electrons. The loss of power at the third harmonic is considered when the ECCD is calculated. Given the conditions of density $(3.4 \times 10^{19} \mathrm{m}^{-3})$ and electron temperature (2.3 keV) at the location of the ECCD, and the power lost at the third harmonic, the driven current is 16 kA and the peak driven current density is 12.2 $\mathrm{A/cm}^2$, compared to bootstrap current density of 17.1 $\mathrm{A/cm}^2$ and equilibrium current density of 75 $\mathrm{A/cm}^2$ at the time analyzed for Fig. 2 (6315 ms).

The history of an example discharge showing prevention of the 2/1 NTM with β very near the stability limit is in Fig. 3. In this discharge, the EC power was applied at *t*=4500 ms, while β was still rising [Fig. 3(e)]. The saturated $n = 2$ mode that is characteristic of hybrid mode discharges appears earlier [Fig. 3(d)]. As β continues to increase, the PCS makes small adjustments to the toroidal field to maintain the current drive at the minor radius of the $q = 2$ surface. The difference between the calculated minor radius of the current drive and the calculated $q = 2$ radius was kept small compared to the radial width of the current drive layer. Good energy confinement was maintained, and normalized beta was sustained for more than one second at the no-wall kink stability limit of $\beta_T \approx 4.1\%$ and $\beta_N \approx 3.2$. The estimate of the no-wall limit shown in Fig. 3(e) as
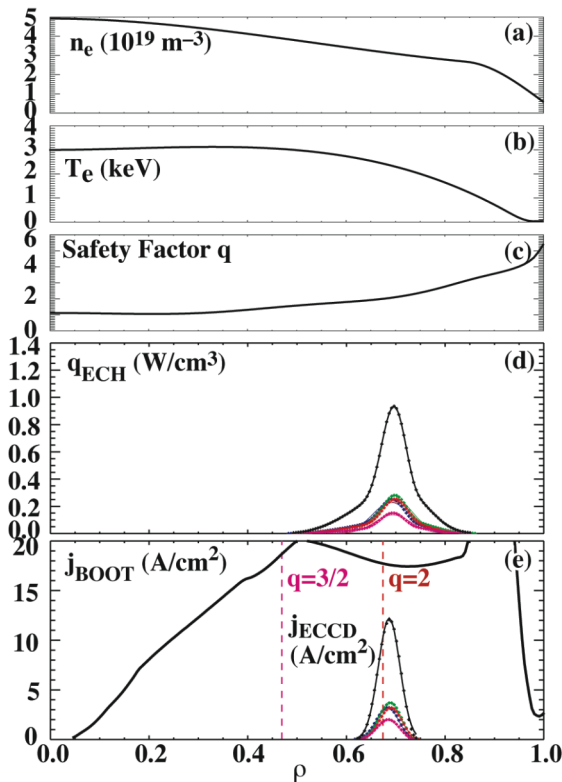

FIG. 2. Profiles as a function of normalized minor radius ρ. (a) Plasma density, (b) electron temperature, (c) safety factor *q,* (d) power density due to EC wave absorption, and (e) ECCD current density profile for each of the four EC systems (colored) and the total (black) and, for comparison, the bootstrap current density profile. Profiles are taken at 6315 ms for shot 122907.
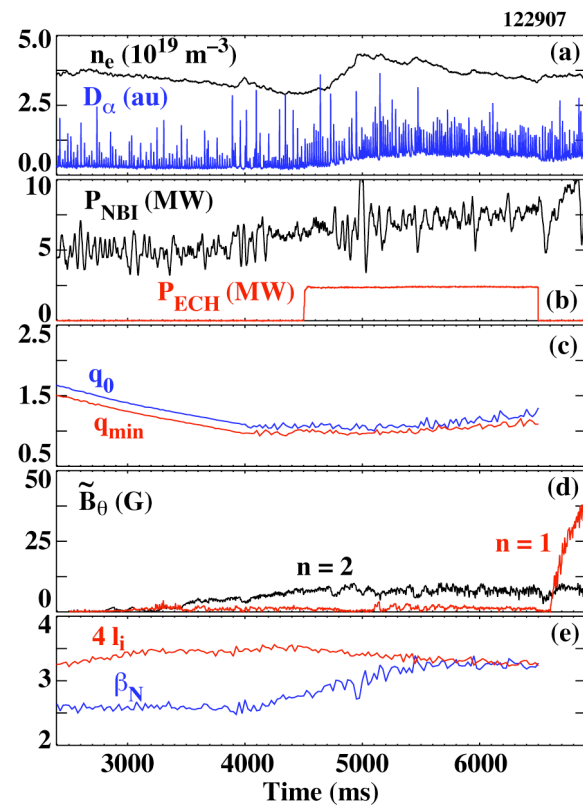

FIG. 3. Time history of plasma behavior. (a) line-averaged density and D_α emission, (b) ECH power and time-averaged neutral beam power, (c) central and minimum value of safety factor q, (d) amplitudes of $n = 2$ and $n = 1$ tearing modes, measured at the outboard midplane wall, (e) normalized beta and four times the internal inductance (an estimate of the beta limit for the ideal $n = 1$ kink mode in the absence of a conducting wall). Traces in (c) and (e) end where the motional Stark effect data stops.

$\beta_N \approx 4 l_i$, with l_i the internal inductance of the plasma, agrees with ideal stability calculations to within about 5%. (Plasma rotation may allow the vacuum vessel wall to stabilize the kink mode at or beyond the no-wall limit.) When the ECCD is turned off at $t =$ 6500 ms, the beta is programmed to maintain the same value. The onset of a 2/1 NTM about 100 ms later, Fig. 3(d), shows that the presence of the ECCD was necessary for the stability of the plasma. This was also clearly seen in comparable discharges without ECCD. Since the ECCD is applied at a rather large minor radius, the heat is not well confined, and the EC power reduces the normalized confinement time H_{89} from 2.35 to 2.0 if it is included in the total heating power. Here, the ECCD is used to increase the stability limit rather than confinement.

Many previous experiments on established NTMs have shown that precise positioning of the current driven by ECCD is crucial to successful suppression of the mode. In this experiment the mode is absent, but the accuracy of the placement of the ECCD is believed to be equally important. In the work on fully grown NTMs, the effects of the continuous co-ECCD very near the rational surface are to replace the loss of the bootstrap current within the island due to the flattening of the pressure gradient within the island and to increase the classical stability (that is, make Δ' more negative). In these experiments only the latter process is in effect when islands aren't present, but the coupling to edge localized modes (ELMs) or the higher order components of the 3/2 mode can generate small islands, so replacing the missing bootstrap current is kept in the modeling of the pre-emptive control. From a theoretical point of view, this experiment is somewhat cleaner than the case with substantial islands, since the effect of the islands on broadening the effective ECCD profile need not be considered. Also, the coupling between modes which has been observed on DIII-D to cause frequency locking between the m=3/n=2 mode at the $q = 3/2$ surface and the 2/1 mode at the $q = 2$ surface is avoided. Finally, the change in Δ' due to the presence of an island need not be considered.

The key problems in devising a closed-loop feedback control system to keep the ECCD on the $q = 2$ flux surface are identifying the location of the rational surface in real space and determining the location of the peak of the ECCD. In these experiments this is done by carrying out reconstructions of the equilibrium in real time, which provides a profile of the safety factor q. The real-time equilibrium reconstructions are carried out by the PCS using information from 26 internal poloidal field measurements from the motional Stark effect diagnostic, as well as a large number of magnetic measurements outside the plasma. The real-time EFIT algorithm obtains a solution to the Grad-Shafranov equation that minimizes the differences between the input signals and the equilibrium. The time required to obtain an equilibrium is about 8 ms, and the solutions obtained are very close to those obtained off-line using the EFIT code with the same input data. However, not as much filtering of the inputs is performed for the real time EFITs as for off-line EFITS, so the results contain a little more scatter. The location in R and Z of the ECCD is calculated for an earlier discharge with similar properties, and the PCS calculates the change needed to B_T in order to bring the R of the peak ECCD into coincidence with the $q = 2$ surface at the same Z. The response time of the toroidal field to the PCS signal is a few hundred milliseconds.

This closed-loop system is effective in keeping the ECCD aligned with its target surface. Figure 4 shows the ECCD profile as a function of time, along with the post-discharge calculation of the minor radius of the $q = 2$ surface. The toroidal field shown in Fig. 4(b) needed to obtain and maintain the alignment is controlled by the PCS based on the real-time reconstructions. Small changes in the calculated q-profile can shift the location of the $q = 2$ surface substantially, so the uncertainty in the $\rho_{q=2}$ surface is of order 0.05. This uncertainty

is addressed in practice by determining $\rho_{q=2}$ empirically, by finding the most effective location of ECCD in similar discharges with 2/1 islands using the automated "search and suppress" procedure to find the optimum value of B_T. The difference between the calculated $\rho_{q=2}$ and the ρ_{ec} for the optimum B_T is added to subsequent real-time calculations of $\rho_{q=2}$. In Fig. 4, after the initial jog to align the ECCD with the rational surface, the changes called for by the PCS are modest. For some discharges like the present one, the toroidal field could be successfully pre-programmed after substantial trial and error, but the result is much less robust. The closed-loop system is much more effective in maintaining correct alignment over a range of conditions.

3. Discussion

These experiments on DIII-D have shown that avoiding the 2/1 NTM by means of ECCD at the $q = 2$ surface can provide stable operation at plasma pressures that would be otherwise unstable. Figure 5 shows the pressure limit for instability to a 2/1 NTM for a group of similar hybrid discharges without ECCD, plotted as a function of ρ_i^*, the ion gyroradius normalized to the minor radius. La Haye [1] has shown that twice the ion banana width is an accurate estimate of the marginal island size for NTM instability. Figure 5 shows that the discharge of Fig. 1 with ECCD is stable where other similar discharges are unstable. It is possible that a discharge like 122907 with ECCD may be stable to β_N above the no-wall β limit, but this has not yet been tested.

Modeling the discharge using the modified Rutherford equation shows that pre-emptive ECCD at the level of discharge 122907
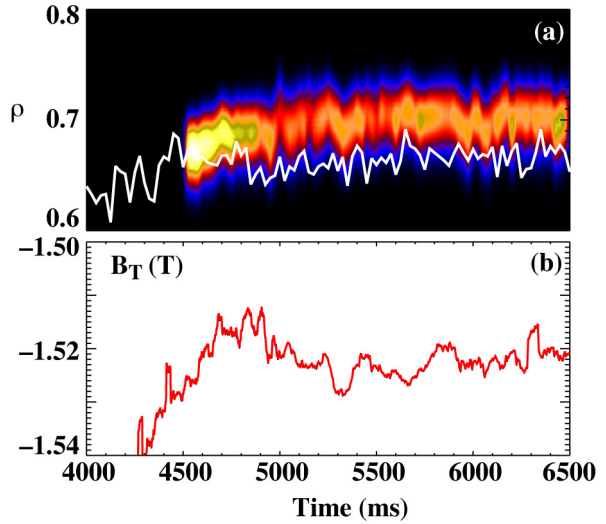

FIG. 4. (a) Profile of ECCD (colored bands) and the minor radius of the $q = 2$ surface calculated from post-discharge reconstruction including MSE data but without pressure data, and (b) toroidal magnetic field controlled by the PCS, as a function of time, for the same discharge as that of Fig. 3. A change in B_T of 0.01 T gives a radial shift of the ECCD location by 0.9 cm.
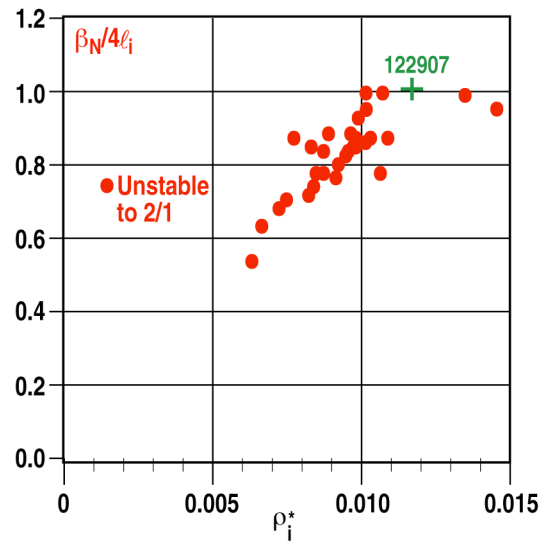

FIG. 5. Pre-emptive ECCD avoids the m/n = 2/1 NTM in Hybrid scenario discharges at the n = 1 no-wall ideal kink beta limit in DIII-D, estimated as $4l_i$.

removes the unstable parameter space. Figure 6 shows the calculated normalized growth rate of the 2/1 NTM as a function of the island width. The upper curve is the growth rate if no ECCD were applied. It shows that a trigger mode of width 2.5 cm is needed for the 2/1 mode to grow, and that if growth takes place the island width will saturate at 14 cm, a very large island which likely would have locked before reaching saturation. The lower curve is for the same discharge but including the effect of ECCD. The ECCD makes Δ' more negative [12],

enhancing the stability, and no island size is unstable. In the model [15] for the curves in Fig. 6, the effect of replacing the missing bootstrap current is included. From experiment, the misalignment of the ECCD $\Delta\rho$ at 6475 ms is $0.38\delta_{EC}$, where δ_{EC} is the FWHM of the ECCD profile. The peak of the ECCD is $0.70\,j_{bs}$, where j_{bs} is the local bootstrap current density. Other qualities which enter the model are $j_{bs}/j_{\parallel} = 0.22$, where $j_{\parallel}$ is a current density characteristic of the equilibrium, the magnetic shear length is 32 cm, and the marginal island width is 3.8 cm. The effect of the ECCD on the classical instability index Δ' is to reduce $r\Delta'$ from -2.0 to -3.8 [16].
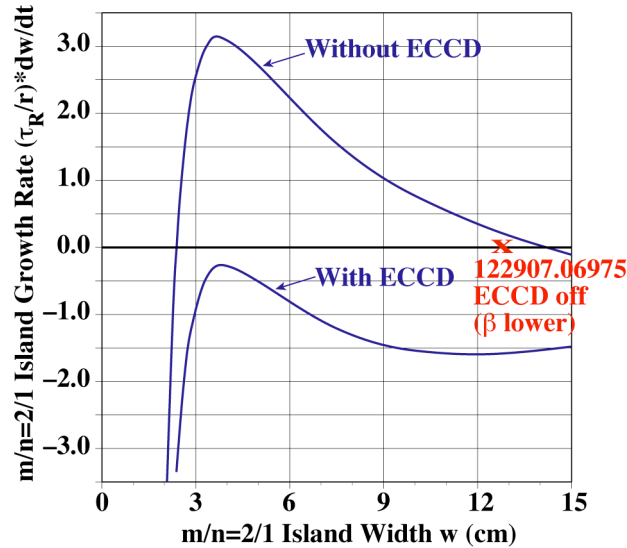

FIG. 6. Modeling for t = 6475 ms in 122907 shows that pre-emptive ECCD makes the growth rate of the 2/1 NTM negative for all island widths. The red x shows the measured saturation island width for the discharge of Fig. 1 after the ECCD is ended and the mode becomes unstable, with the β slightly lower due to the effect of the island on confinement and saturation of the neutral beam power in maintaining β_N.

A very similar discharge, 122906, shows that the condition $\dot{w} < 0$ for all values of w is indeed marginal, as shown in the lower curve of Fig. 6. In 122906, the 2/1 mode is completely stabilized using 2.4 MW of EC power, but when the EC power decreases to 1.75 MW at 5840 ms, the 2/1 mode promptly grows. The reduction in EC power raises the "with ECCD" curve of Fig. 6 so that an unstable range of w is introduced.

4. Conclusions

This work shows that pre-emptive avoidance of the 2/1 NTM by application of ECCD at the $q = 2$ surface avoids many of the problems affecting stabilization of a fully-grown mode. A key benefit is that the locking of a 2/1 NTM to the resistive wall may be eliminated, and it is this locking that leads to disruption, which may be a major concern in a large device like ITER. The key problem with pre-emptive ECCD is getting the ECCD at the correct location, which is difficult to achieve in the absence of the mode. Here we have shown that real-time reconstructions of the equilibria can be used to find and track the flux surface where $q = 2$. A simple model for EC wave propagation and deposition was used by the digital plasma control system to determine the optimum magnitude of the toroidal field giving alignment of the ECCD with the rational surface. (Alignment control in ITER would be done using real-time steerable mirrors.) The resultant improvement in stability can be understood in terms of the

modified Rutherford equation including the effects of the localized ECCD on both the classical stability index and replacing the missing bootstrap current. Future experiments will test whether the β can be raised above the no-wall limit.

References

[1]   LA HAYE, R.J., PRATER, R., BUTTERY, R.J., *et al.,* Nucl. Fusion **46** (2006) 451.
[2]   LUCE, T.C., WADE, M.R., FERRON, J.R., Phys. Plasmas **11** (2004) 2627.
[3]   HEGNA, C., and CALLEN, J., Phys. Plasmas **4**, 2940 (1997).
[4]   ZOHM, H., Phys. Plasmas **4**, 3433 (1997).
[5]   GANTENBEIN, G., ZOHM, H., GIRUZZI, G., *et al.,* Phys. Rev. Lett. **85**, (2000) 1242.
[6]   PRATER, R., LUCE, T.C., PETTY, C.C., *et al.,* Fusion Energy 2000 (Proc. 18th Int. Conf. Sorrento, 2000) (Vienna: IAEA)
       http://www.iaea.org/programmes/ripc/physics/fec2000/html/node114.htm.
[7]   ISAYAMA, A., KAMADA, Y., IDE, S., *et al.,* Plasma Phys. Control. Fusion **42** (2001) L37.
[8]   PETTY, C.C., LA HAYE, R.J., LUCE, T.C., *et al.,* Nucl. Fusion **44** (2004) 243.
[9]   GANTENBEIN, G., *et al.,* Proc. 30th EPS Conf. on Plasma Physics, St Petersburg, Russia, Vol. 27A (2004) p. 1.120.
[10] PRATER, R., LA HAYE, R.J., LOHR, J., *et al.*, Nucl. Fusion **43** (2003) 1128.
[11] LA HAYE, R.J., HUMPHREYS, D.A., FERRON, J.R., *et al.,* Nucl. Fusion **45** (2005) L37.
[12] PLETZER, A., and PERKINS, F.W., Phys. Plasmas **6** (1999) 1589.
[13] RUTHERFORD, P.H., Phys. Fluids **16** (1973) 1903.
[14] NAGASAKI, K., ISAYAMA, A., IDE, S., Nucl. Fusion **43** (2003) L7.
[15] LA HAYE, R.J., *et al.*, this conference.
[16] WESTERHOF, E., Nucl. Fusion **30** (1990) 1143.